# Molecular Tagging Velocimetry development for in-situ measurement in High-Temperature Test Facility

Matthieu A. André and Philippe M. Bardet
*The George Washington University: 800 22nd St NW, Washington, DC, 20052, bardet@gwu.edu*

Ross A. Burns
*National Institute of Aerospace: Hampton, VA, 23666*

Paul M. Danehy
*NASA Langley Research Center: Hampton, VA 23681*

## INTRODUCTION

The High Temperature Test Facility, HTTF, at Oregon State University (OSU) is an integral-effect test facility designed to model the behavior of a Very High Temperature Gas Reactor (VHTR) during a Depressurized Conduction Cooldown (DCC) event. It also has the ability to conduct limited investigations into the progression of a Pressurized Conduction Cooldown (PCC) event in addition to phenomena occurring during normal operations. Both of these phenomena will be studied with in-situ velocity field measurements. Experimental measurements of velocity are critical to provide proper boundary conditions to validate CFD codes, as well as developing correlations for system level codes, such as RELAP5 (http://www4vip.inl.gov/relap5/). Such data will be the first acquired in the HTTF and will introduce a diagnostic with numerous other applications to the field of nuclear thermal hydraulics.

A laser-based optical diagnostic under development at The George Washington University (GWU) is presented; the technique is demonstrated with velocity data obtained in ambient temperature air, and adaptation to high-pressure, high-temperature flow is discussed.

## MOLECULAR TAGGING VELOCIMETRY TECHNIQUE

Molecular tagging velocimetry (MTV) is a non-intrusive optical diagnostic to measure velocity of fluids. It is a time-of-flight measurement technique, which utilizes molecules as tracers instead of macroscopic particles as in particle image velocimetry (PIV) or particle tracking velocimetry (PTV). MTV has been used both in gas- and liquid-phase fluids. In the gas phase, several techniques exist to "tag", or mark, the molecules of interest; see an introduction in [1]. The most common measurement scheme involves the creation or excitation a radical chemical species and subsequently tracking its motion with planar laser-induced fluorescence (PLIF). The first step in designing an MTV system is to identify the proper tracers and marking scheme to employ for a given environment.

For the HTTF conditions, a series of potential tracers has been identified. One important criterion used in the selection process was the lifetime of the chosen chemical species; the selected species had to survive long enough in this high-pressure (several atmospheres), high-temperature (700 to 1000 K) environment. Fortunately, the test gas is inert, which promotes long tracer lifetime and increases the number of potential choices for use with the MTV technique. Suitable species that have been identified include $N_2O$ [2], $NO_2$ [3], Kr [4], $O_2$ [5], $N_2$ [6], and $H_2O$ [5]. For these tracers, with the exception of $N_2$ and Kr, the excitation process involves first generating a radical species with one laser system, the so-called "write pulse". With a second laser system, typically involving a tunable dye laser, PLIF is performed on the previously generated radicals one or more times. These "read pulses" allow for the detection of the position of the tracers created during the write pulse at both the initial and one or more delayed times. A flexible laser system was built at GWU, enabling the testing of 3 of the 6 markers identified. Results are presented for using $H_2O$ (to create OH* radicals), which is presently the favored scheme for the MTV system in the HTTF due to its non-toxicity, ease to add to the test gas, and relatively long lifetime at the current operating conditions. Only small concentration of $H_2O$ is necessary, which will lead to limited corrosion inside the pressure vessel.

The present hydroxyl tagging velocimetry (HTV) system is composed of an excimer laser (write pulse), a dual-pulse tunable dye laser (read pulses) and an intensified CCD camera (imager). The excimer laser, dye laser, and the two pump lasers are mounted on a cart (shown in figure 1) to permit easy transport to the HTTF at OSU after the technique has been optimized at GWU. A diagram of this laser system is shown in figure 2. The excimer outputs a 14 mJ/pulse beam at 193 nm to photo-dissociate $H_2O$ into OH* radicals. Photo-dissociation of $H_2O$ into OH* using a 193 nm beam is relatively inefficient (1%) at ambient temperature. High temperature vapor, as encountered in the HTTF conditions, is already vibrationally excited, and will be dissociated much more efficiently at 193 nm and higher temperatures: 6% 750K or 15% at 1200K [5].

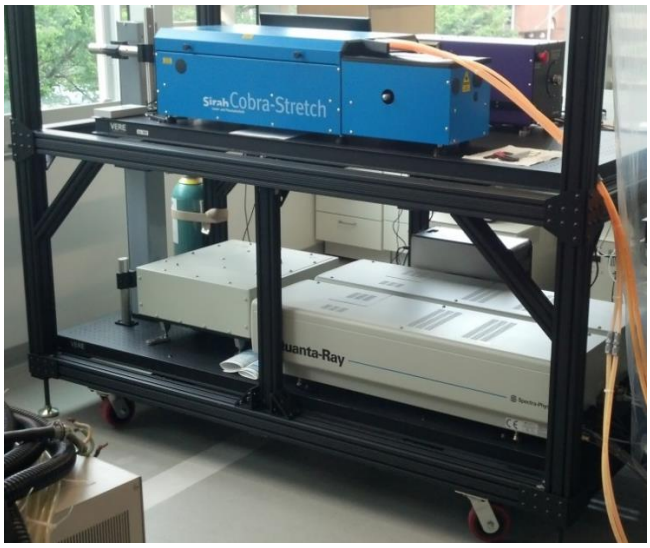


Figure 1: Lasers mounted on the cart. Dye laser (blue) and excimer (purple) are on the top breadboard, while pump lasers and beam combiner are on the bottom breadboard. A periscope brings the Nd:YAG beams to the top breadboard.

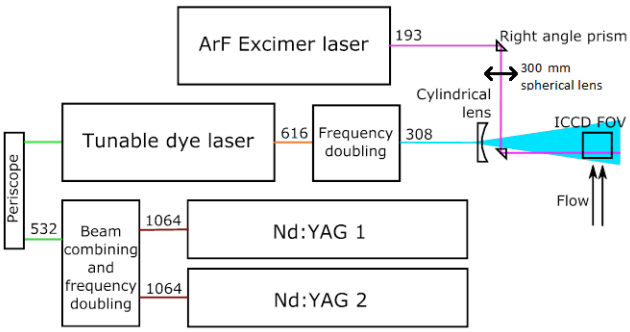


Figure 2: Setup of the lasers used for "write" and "read" pulses. Wavelengths are given in nm. ICCD FOV stands for Intensified CCD field of view.

The output of two frequency-doubled Nd:YAG lasers (10 Hz, 0.5 J/pulse, 532 nm) are combined to pump a dye laser. By using two Nd:YAG lasers (with a short delay between pulses) to pump the tunable dye laser, the latter can operate as a dual-pulse system. This is particularly important to conduct time-of-flight measurements. The first pulse measures the initial beam position, just after the write pulse, while the second captures the displacement of the radicals at a later time that is optimized to maximize accuracy. This dual-pulse configuration allows correcting for potential beam wandering of the write laser, and hence leads to higher accuracy measurements in comparison to using only a single read pulse. Using rhodamine dyes and a frequency-doubling BBO crystal, $A^2\Sigma^+$-$X^2\Pi$ transitions of the OH* radical can be excited. The present work focuses on exciting the (0,0) and (1,0) vibrational transitions, around 308 and 283 nm, respectively.

Fine tuning of the PLIF system wavelength maximizes the fluorescence signal. The $Q_1(3)$ rotational transition in the (0,0) band at 308.154 nm is used for resonant fluorescence in the data presented here. In this setup, fluorescence emission is around the same wavelength as the excitation, which prevents the use of spectral filters to remove scattered laser light. Work is also ongoing using the $Q_1(9)$ and $Q_2(8)$ absorption lines in the (1,0) band around 283.925 nm, which allows using spectral filters to remove scattered light and minimize the need to pre-process the images before extracting the displacement. However, the absorption at the (1,0) transition is lower compared to the (0,0) transition, which results in a comparatively weaker signal.

The fluorescence signal from the read pulses is recorded with a time-gated image intensifier coupled to a 12-bit CCD camera. A UV-transmitting lens is mounted on the image intensifier providing a resolution of 21.4 pixels/mm. The gate time of the latter can be decreased down to 10 ns and temporally centered on the PLIF signal to effectively suppress the background noise. The CCD camera is connected to a workstation through a Firewire interface which allows images to be written directly to hard drive, enabling to record extended duration of data (10 hours at 2×10 Hz). Instruments are synchronized using a pulse generator (Berkeley Nucleonics 575) with an accuracy of 250 ps and are monitored with a high-speed digital oscilloscope (Agilent MSOX-3054A).

## VELOCITY MEASUREMENT RESULTS

The HTV technique is demonstrated at ambient temperature and pressure. Compressed air is bubbled through water and exits a 15.8 mm inner diameter vertical pipe, forming a round jet in which velocity is to be measured.

The excimer beam is focused to a line perpendicular to the jet centerline. The dye laser beam is shaped into a vertical sheet that contains the path of the excimer beam, see Fig. 2. At $t$ = 0 s, the excimer laser is pulsed to create a horizontal line of OH* radicals located 25 mm downstream of the pipe exit. The tracers are then convected by the flow and their positions are read some time later using a 3.5 mJ dye laser pulse. The image intensifier is gated for 100 ns to capture the OH* fluorescence and amplifies the signal to a level detectable by the CCD camera. Though the images are contaminated by scattered light due to airborne particles, this effect is suppressed through image processing. Figure 3 presents processed PLIF images taken at three different times after OH* creation. The first, second, and third images correspond to $t$ = 10, 110, and 210 µs, respectively. In the first frame, the PLIF signal is strong and very close to a straight line, indicative of the short time delay between the write and the read pulses. As the probe time was increased, the line of fluorescence convected visibly (see images 2 and 3 in figure 3), with the largest displacements occurring at the jet centerline ($x$ = 0 mm) where the velocity was

expected to be highest. A few general observations can be made regarding this progression of images. There is a distinct trend of decreasing signal-to-noise ratio (SNR) as the time delay was increased. There are two primary reasons for this trend; first, the signal intensity decreases as the concentration of OH* radicals is reduced by recombination with ambient species. Second, molecular diffusion causes the hydroxyl radicals present to become interspersed with surrounding molecules, causing the line to spread out and decreasing the peak signal intensity. It is anticipated that the high-pressure environment present in the HTTF will reduce the effects of molecular diffusion considerably, which will allow for higher SNRs at similar or potentially longer time delays.

Another trend apparent from these images is that the OH* fluorescence is considerably stronger near the core of the jet, caused both by the increased concentration of water vapor and the focusing of the excimer laser beam through this region (thus producing higher concentrations of hydroxyl). The consequence of these effects is a further reduction in SNR near the edges of the jet and surrounding fluid. While the former of these two causes is not anticipated to be problematic in the HTTF, where there will be a uniform distribution of water vapor, the latter effect will still be present.

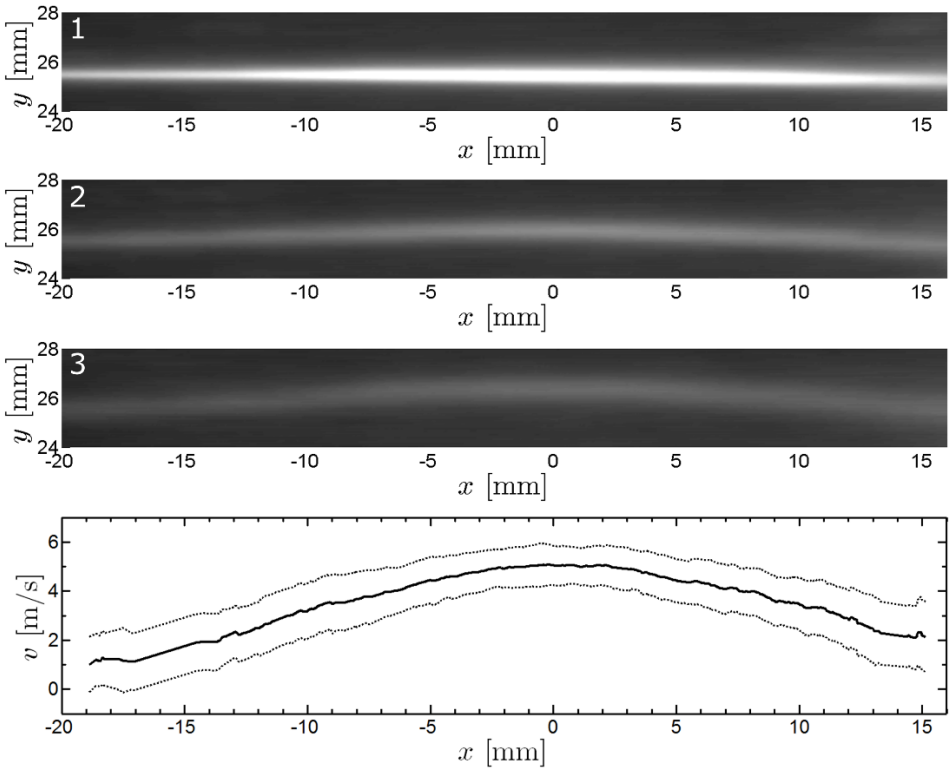


Figure 3: Mean OH-PLIF images recorded 10μs (1), 110μs (2), and 210μs (3) after OH radicals are formed with the excimer laser. Each image is obtained by averaging a minimum of 100 raw images. The velocity profile is computed using a custom curve-fitting algorithm between image sets 1 and 2. Uncertainty bounds are taken to be one standard deviation of the measured single-shot velocity distribution.

The results of the velocity calculations are shown in the final pane of Fig 3. Line displacements in the vertical direction are calculated using a custom curve-fitting algorithm to identify the centroid of the intensity distribution. Due to the low signal-to-noise ratio in the instantaneous images, column binning was performed over a region 64 pixels (~3 mm) wide. Additional filters were then applied to remove erroneous fits and data in which the SNR was unacceptably low. Finally, the mean profiles were conditioned on there being a sufficient number of viable samples (20) to construct the desired velocity distributions. It was found that the inclusive velocity range for the velocity profile is between 1 and 5 m/s. This is an important result in considering the application of HTV to the HTTF, where the peak velocities are expected to be on the order of a few m/s. The technique is thus capable of resolving velocities at this order of magnitude, owing to the long time delays, which are afforded by using OH* as a tracer.

Addressing the accuracy, precision, and overall uncertainty in the measurement was difficult in these preliminary measurements due to the low number of samples available for calculation. However, some assessment of the measurement precision was made based on both the measured variance in the velocity distribution as well as past works in the MTV literature. Unfortunately, no assessment of the measurement accuracy could be made for

the current experiments, since there was no direct basis for comparison to a known or accepted measurement available. The measurement precision (based on one standard deviation of a series of repeated measurements) was found to vary considerably with both signal-to-noise ratio and delay. Near the core of the jet, where the SNR was highest, the precision was approximately 0.8 m/s for the 1→2 velocity calculations ($\Delta t$ = 100 $\mu$s), 1.4 m/s for the 2→3 calculations ($\Delta t$ = 100 $\mu$s) and 0.6 m/s for the 1→3 calculations ($\Delta t$ = 200 $\mu$s). In contrast, near the edges of the jet, where the SNR was lower, a similar variation was observed: the precision for the 1→ 2 velocity calculations was found to be 1.0 m/s in these regions, while the 2→3 and 1→3 calculations yielded 1.7 m/s and 0.8 m/s, respectively. It was thus observed that precision worsened with decreasing SNR, while simultaneously being improved with longer time delays. The data of Bathel, et al. [7], obtained from a similar measurement system and technique, provides a reference against which to assess the trends in precision. They found the measurement precision to improve inversely with the time delay used. Extrapolating their results to the conditions of the current study, it can be estimated that the measurement precision for the 1→2 velocity profile should lie in the range 0.75 to 1 m/s in the core of the jet, and in excess of 1.25 m/s in the tails of the jet where the SNRs were substantially lower. In considering the other two velocity calculations, the estimated precision for the 2→3 calculation should lie in the range of 1.25 to 1.5 m/s in the jet core, while the precision for 1→3 calculations should lie the range of 0.45 to 0.7 m/s. In comparing these estimations to the current measured precision, the values are consistent, suggesting that the methodology used in measuring the velocities is similarly precise to other available methods.

It is important to note that these estimations of the measurement precision still represent a substantial fraction of, or in some cases exceed, the measured velocities, particularly in the ambient regions where the gas is nominally quiescent. Improving the measurement precision will require an increase in the observed signal-to-noise ratios and/or further increasing the temporal delay between images. However, increasing the time delay has other consequences in terms of spatial and temporal resolution. The spatial resolution of MTV scales, at first order, with the recorded distance traveled by the tracer molecules. Hence, increasing the temporal delay improves the precision, but also decreases the spatial and temporal resolution. Selecting the optimal delay will require more development to assess all the potential circumstances influencing the measurement quality.

Future work will focus on improving the overall quality of the preliminary measurements herein presented, further assessment of the measurement system, and ultimately the optimization of the diagnostic technique for its eventual application to the HTTF at OSU. Efforts are underway to create a small-scale lab environment to recreate the actual thermodynamic conditions expected in the HTTF. Furthermore, future measurements will seek to more effectively assess the precision, accuracy, and uncertainty of the velocity measurements.

## CONCLUSIONS

MTV has been proposed to instrument the HTTF at OSU. A moveable laser system has been built at GWU and demonstrated with OH* tracers at ambient temperature and pressure. OH* radicals are created with an excimer laser and tracked using PLIF, allowing for the measurement of a flow velocity profile using time-of-flight calculation. Preliminary measurements were made in a low-speed jet; average velocities ranging from -0.5 to 4.5 m/s were resolved, which is consistent with the expected velocities in the HTTF. The measurement precisions were determined to be limited by the low SNRs of the current experimental data. However, it is expected that the photo-dissociation efficiency and PLIF signal strength will increase considerably in the hotter HTTF conditions. Further assessment and optimization of the MTV technique will be performed at GWU, including the use of a new high-pressure, high-temperature chamber currently under construction at GWU.

## ACKNOWLEDGEMENTS

This project was supported by a DOE NEUP grant to Dr. Bardet.

## REFERENCES

1. Springer Handbook of Experimental Fluid Mechanics, ed. Topea, Yaris, Foss, ch. B.5.4.
2. ElBaz, A. M., and R. W. Pitz. "$N_2O$ molecular tagging velocimetry." Applied Physics B 106.4 (2012): 961-969.
3. Danehy, Paul M., et al. "Flow-tagging velocimetry for hypersonic flows using fluorescence of nitric oxide." AIAA journal 41.2 (2003): 263-271.
4. Parziale, N. J., Smith, M. S., and Marineau, E. C. "Krypton tagging velocimetry of an underexpanded jet." Applied Optics, 54.16 (2015): 5094-5101.
5. Pitz, Robert W., et al. "Unseeded molecular flow tagging in cold and hot flows using ozone and hydroxyl tagging velocimetry." Measurement Science and technology 11.9 (2000): 1259.
6. Danehy, Paul M., et al. "Three-component velocity and acceleration measurement using FLEET." 30th AIAA Aerodynamic Measurement Technology and Ground Testing Conference, June 2014
7. B. Bathel, P. M. Danehy, C. Johansen, S. Jones, C. Goyne, "Hypersonic Boundary Layer Measurements with Variable Blowing Rates Using Molecular Tagging Velocimetry," Paper AIAA-2012-2886, 28th Aerodynamic Measurement Technology, Ground Testing, and Flight Testing Conference, New Orleans, Louisiana, June 25-28, 2012